

# Mafic eclogites from the Valosio crystalline massif (Ligurian Alps, Italy)

Autor(en): **Messiga, Bruno / Tribuzio, Riccardo / Scambelluri, Marco**

Objekttyp: **Article**

Zeitschrift: **Schweizerische mineralogische und petrographische Mitteilungen  
= Bulletin suisse de minéralogie et pétrographie**

Band (Jahr): **72 (1992)**

Heft 3

PDF erstellt am: **05.08.2024**

Persistenter Link: <https://doi.org/10.5169/seals-54919>

## **Nutzungsbedingungen**

Die ETH-Bibliothek ist Anbieterin der digitalisierten Zeitschriften. Sie besitzt keine Urheberrechte an den Inhalten der Zeitschriften. Die Rechte liegen in der Regel bei den Herausgebern.

Die auf der Plattform e-periodica veröffentlichten Dokumente stehen für nicht-kommerzielle Zwecke in Lehre und Forschung sowie für die private Nutzung frei zur Verfügung. Einzelne Dateien oder Ausdrucke aus diesem Angebot können zusammen mit diesen Nutzungsbedingungen und den korrekten Herkunftsbezeichnungen weitergegeben werden.

Das Veröffentlichen von Bildern in Print- und Online-Publikationen ist nur mit vorheriger Genehmigung der Rechteinhaber erlaubt. Die systematische Speicherung von Teilen des elektronischen Angebots auf anderen Servern bedarf ebenfalls des schriftlichen Einverständnisses der Rechteinhaber.

## **Haftungsausschluss**

Alle Angaben erfolgen ohne Gewähr für Vollständigkeit oder Richtigkeit. Es wird keine Haftung übernommen für Schäden durch die Verwendung von Informationen aus diesem Online-Angebot oder durch das Fehlen von Informationen. Dies gilt auch für Inhalte Dritter, die über dieses Angebot zugänglich sind.

## Mafic eclogites from the Valosio crystalline massif (Ligurian Alps, Italy)

by Bruno Messiga<sup>1</sup>, Riccardo Tribuzio<sup>1</sup> and Marco Scambelluri<sup>2</sup>

### Abstract

The mafic layers outcropping in the Valosio Crystalline Unit (Ligurian Alps) record an early Alpine-type eclogite event. The eclogite assemblage consists of omphacite, garnet, rutile, paragonite, epidote and quartz. Temperatures of about  $530 \pm 50$  °C for a minimum 1.2 GPa pressure have been evaluated on the basis of common geothermobarometers. Moreover, paragonite stability indicates that pressure did not exceed 2.0 GPa.

The eclogite event is successively overprinted by three retrograde stages. In the first one, glaucophane crystallized after omphacite, and the eclogitic garnet (grt<sub>1</sub>) developed thin rims of Ca-richer neoblastic garnet (grt<sub>2</sub>).

The second stage is represented by the development of symplectites at the expense of omphacite. Microtextures within the symplectite domains indicate time dependent transformations from clinopyroxene-plagioclase (P ca. 0.9 GPa) to hornblende-plagioclase assemblages (P 0.4 GPa, T = 450–500 °C). Besides, the garnet porphyroblasts are replaced by thin amphibole coronas with a pargasite-hornblende compositional range, whereas glaucophane develops hornblende rims.

The third stage is characterized by the development of actinolite-albite symplectites. The Valosio eclogites display relevant paragenetic and evolutionary similarities with the "cold" eclogite unit of the Dora Maira massif. The inferred P-T path for the Valosio eclogites supports a mechanism of adiabatic upwelling.

*Keywords:* Eclogite, metamorphic evolution, mineral chemistry, thermobarometry, Valosio massif, Ligurian Alps, Italy.

### Introduction

The crystalline massifs of the Ligurian Alps are currently interpreted as scattered fragments of pre-mesozoic continental crust (VANOSI, 1980; VANOSI et al., 1980). They mainly consist of ortho- and paragneisses interlayered with minor amphibolites and calc-silicate rocks (MESSIGA, 1981; DEL MORO et al., 1981; CORTESOGNO, 1984). According to their structural location and metamorphic history, the slices of continental crust in the Ligurian Alps (Fig. 1) are either ascribed to the Briançonnais Domain (Calizzano-Savona and Arenzano massifs), or to the Penninic Zone (Valosio massif; CHIESA et al., 1975; VANOSI et al., 1984).

The Briançonnais Crystalline Basement (hereafter BCB) still retains some primary stratigraphic relationships with the post-Westphalian sedi-

mentary cover (VANOSI et al., 1984). A peculiar feature of the BCB continental slices is the widespread occurrence of mafic pods locally preserving the relics of a Variscan garnet-clinopyroxene eclogite assemblage. The high pressure (T ca. 650 °C, P > 1.2 GPa) paragenesis is overprinted by a sequence of decompressional assemblages towards amphibolite facies conditions (MESSIGA, 1981; CORTESOGNO, 1984; CORTESOGNO and GAGGERO 1988; MESSIGA et al., 1992). The Variscan events in BCB metamorphites were lately overprinted by the Alpine metamorphism (MESSIGA et al., 1981; MESSIGA, 1987). In particular, the mafic rocks from the BCB locally display a lawsonite + glaucophane + Na-clinopyroxene + sphene Alpine assemblage, indicative of a blueschist pressure climax (MESSIGA et al., 1975; MESSIGA, 1987).

The Valosio massif is tectonically overlain by the high pressure Alpine metaophiolites of the

<sup>1</sup> Dipartimento di Scienze della Terra, Università di Pavia, via A. Bassi, 4, I- 27100 Pavia, Italy.

<sup>2</sup> Dipartimento di Scienze della Terra, Università di Genova, Corso Europa, 26. I-16132 Genova, Italy.

Voltri massif and records an Alpine eclogite equilibration (FORCELLA et al., 1973; CORTESOGNO, 1984). Mafic rocks occurring in metaophiolites as well as in the Valosio continental crust exhibit in fact a widespread omphacite-garnet assemblage (ERNST, 1976; MESSIGA et al., 1983; MESSIGA and SCAMBELLURI, 1991). On this ground, the Valosio massif was interpreted as the southernmost unit of crystalline basement melanged with the Penninic ophiolites, such as the Mt. Rosa, Gran Paradiso and Dora-Maira massifs of the Western Alps (FORCELLA et al., 1973; CHIESA et al., 1975; VANOSSI et al., 1984).

In recent years, the P-T paths and histories of eclogites from the BCB and the Voltri massif have been thoroughly reconstructed in order to define the tectonic mechanisms ruling the uplift processes of these units (MESSIGA et al., 1983, 1992; MESSIGA, 1987; MESSIGA and SCAMBELLURI, 1991). Concerning the Valosio massif, despite the

papers of CORTESOGNO (1984) and CABELLA et al. (1991), detailed data on its full metamorphic evolution are still lacking.

The aims of this paper are: – firstly, to show the presence of a widespread eclogite facies assemblage in mafic rocks; – secondly, to decipher their retrograde history; – finally, to compare the petrological features and P-T path of the Valosio eclogites with the metamorphic history of other Ligurian eclogites.

In order to develop a homogeneous dataset of microtextural and petrological observations, this study builds on the same methodological approach used in the investigation of the eclogites from the Voltri massif and the Savona crystalline massif (MESSIGA and SCAMBELLURI, 1991 and MESSIGA et al., 1992, respectively). According to RUBIE (1990), eclogites retain widespread evidence of disequilibrium microtextures such as: – relics of precursor minerals; – development of "mosaic equilibrium"; – reaction coronas. Metamorphic reactions occur mainly in the presence of catalytic factors, such as grain size reduction, fluid infiltration and deformation. Segments of the whole evolution are indicated either by reactions localized at grain boundaries, or by pseudomorphic replacements of precursor minerals (MESSIGA and SCAMBELLURI, 1991; MESSIGA et al., 1992). This leads to complex and sometimes univocal microtextural interpretations. For these reasons microtextures have been investigated at different scales and employing optical and scanning electron microscopes. Electron microprobe data have been produced only on selected microtextures of known relative age. Particular efforts have also been devoted to the resolution of fine-grained microtextures, such as symplectites. The latter represent the occurrence of reactions running over a short time span, or under kinetically unfavoured environment.

### The Valosio massif

The Valosio massif outcrops along the northern sector of the Voltri massif, over a 2.86 km<sup>2</sup> area (BRUNO, 1965; BELLINI, 1966; FORCELLA et al., 1973; CABELLA et al., 1991). It is bounded by steep normal faults of Oligo-Miocene age directed east-west. The Valosio massif retains a former thrust surface marking the contact with the overlaying Voltri massif metaophiolites. Besides the mafic rocks, two other main lithotypes characterize the Valosio massif: gneisses and calc-silicate rocks.

Gneisses are generally foliated and augen textured. Their mineralogy is defined by quartz ribbons, augen K-feldspar, muscovite, calcite,

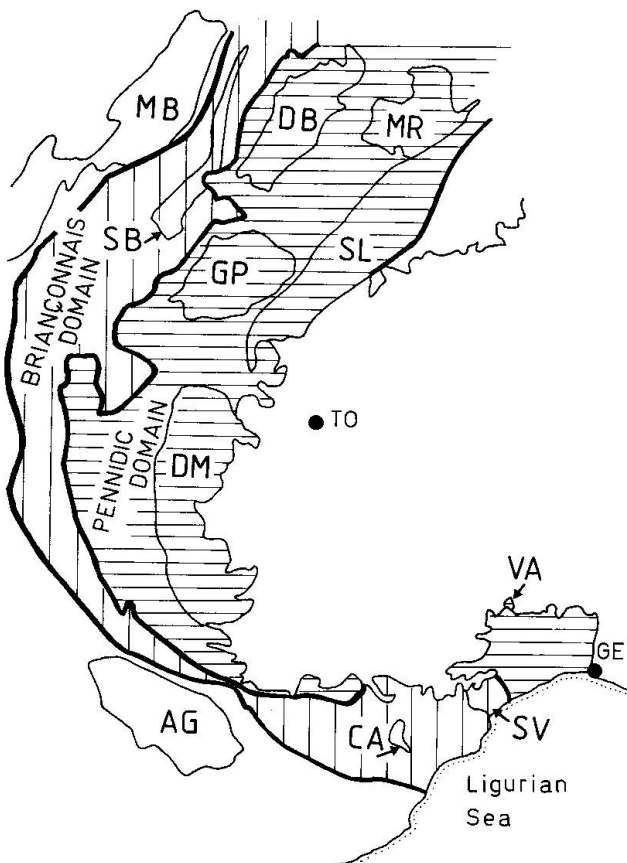


Fig. 1 Simplified sketch map of Western Alps, indicating the Penninic Domain (horizontal ruled area) and Briançonnais Domain (vertical ruled area). The main crystalline units are: Mt. Bianco (MB), Dent Blanche (DB), Mt. Rosa (MR), Saint Bernard (SB), Gran Paradiso (GP), Sesia Lanzo (SL), Dora Maira (DM), Argentera (AG), Calizzano (CA), Savona (SV), and Valosio (VA). TO = Torino, GE = Genova.

zoisite, and minor amounts of biotite and garnet; accessory phases are magnetite, zircon, apatite and zoisite. In particular, the gneiss sequence consist of alternating quartzites and micaschists layers: relative to quartzites, micaschists are characterized by an increase in modal garnet and mica.

Calc-silicate rocks are generally interbedded within both gneisses and mafic rocks. When present within gneisses, the calc-silicate rocks consist of abundant calcite, muscovite, chlorite, zoisite, garnet and quartz. On the contrary, calcite, garnet, tremolite, diopside and sphene characterize the assemblage of the calc-silicate rocks when interbedded in mafic rocks.

### Petrography<sup>1</sup>

Mafic rocks from the Valosio massif are foliated eclogites consisting of omphacite, garnet, paragonite, epidote, rutile, carbonates and quartz (Fig. 2A). Omphacite, garnet, paragonite and epidote display a strong preferred orientation and define the eclogite shear foliation. Garnet porphyroblasts display several solid inclusions, some of which are "multiphase" aggregates. At the garnet cores (grt<sub>1</sub>), the inclusion trails define a straight foliation which gently bends near the rims. A textural "unconformity" truncating the inclusion trails represents the contact between the garnet cores and an external rim of neoblastic, inclusion-free garnet (grt<sub>2</sub>). Garnet porphyroblasts are also dissected by veins filled with retrograde minerals.

The post-eclogitic history is marked by the static development of retrograde minerals either as post-kinematic porphyroblasts, or as symplectitic aggregates, or as coronas and veins which overgrow and/or crosscut the eclogite fabric. Random glaucophane porphyroblasts develop after the eclogite foliation, sometimes retaining cores of relic omphacite. On the other hand, green amphibole develops either in coronas around garnet, or as rims after glaucophane; the occurrence of green amphibole as porphyroblast is restricted to more retrogressed domains.

#### *Symplectites*

Different symplectites are related to the breakdown reactions of omphacite and glaucophane. Symplectites replacing omphacite start to grow along grain boundaries by exsolution re-

action proceeding inwards, as suggested by omphacite relics within symplectite aggregates.

Generally, two different symplectite-types result from the omphacite breakdown. The first (Symp 1) consist of diopside and plagioclase, the second (Symp 2) of green hornblende and plagioclase. Symp 1 occurs in microdomains preserving several omphacite relics and is characterized by diopside/plagioclase lamellae not exceeding 3 µm (Fig. 2C). Only in few cases lamellae develop parallel to rational planes; more frequently, they display globular microtextures. Symp 2 consists of hornblende and plagioclase and is characterized by an increase in the lamellar interspace (up to 10 µm) and globular microtexture (Fig. 2D). Frequently, hornblende lamellae develop rational boundaries according to the crystallographic amphibole shape. The time relationships among the two symplectites result from the presence of relic portions of diopside-plagioclase symplectites inside the hornblende-plagioclase ones. Modally, Symp 2 exceeds Symp 1.

Late tremolite-albite symplectite (Symp 3) may also develop at the expense of omphacite. Actinolite-albite symplectites (Symp 3), however, generally grow at the expense of glaucophane. In particular, they are characterized by an increase in the feldspar/amphibole modal ratio with respect to both Symp 1 and Symp 2.

#### *Coronas*

Green amphibole coronas develop around garnet and glaucophane. The amphibole bounding garnet is zoned, with a thin rim of blue-green amphibole (about 10 µm) close to the garnet. On the other hand, the green amphibole rimming glaucophane relic is optically unzoned.

The omphacite-garnet boundary is marked by reaction rims of bluish-green amphibole (Fig. 2E). Similarly, within garnet porphyroblasts bluish-green amphibole rims develop between the omphacite inclusions and host garnet (Fig. 2B). Colourless zoisite is commonly rimmed by epidote, whereas coarse rims of sphene develop around rutile. Epidote rims are also developed on paragonite (Fig. 2F).

#### *Multiphase inclusions in garnets*

A peculiar feature of garnet cores (grt<sub>1</sub>) is the occurrence of several mono- or multiphase solid inclusions. Omphacitic clinopyroxene, paragonite, epidote and rutile are the most frequent inclusions. Another relevant microtextural aspect is that the multiphase inclusions are connected to each other by blue-green amphiboles-, plagioclase- and, sometimes, calcite-bearing veins. When veins are abundant, garnet grains display a

<sup>1</sup> Mineral abbreviations according to KRETZ (1983); moreover, Bar = barroisite; Prg = pargasite; Sad = sadanagaite; Win = Winchite.

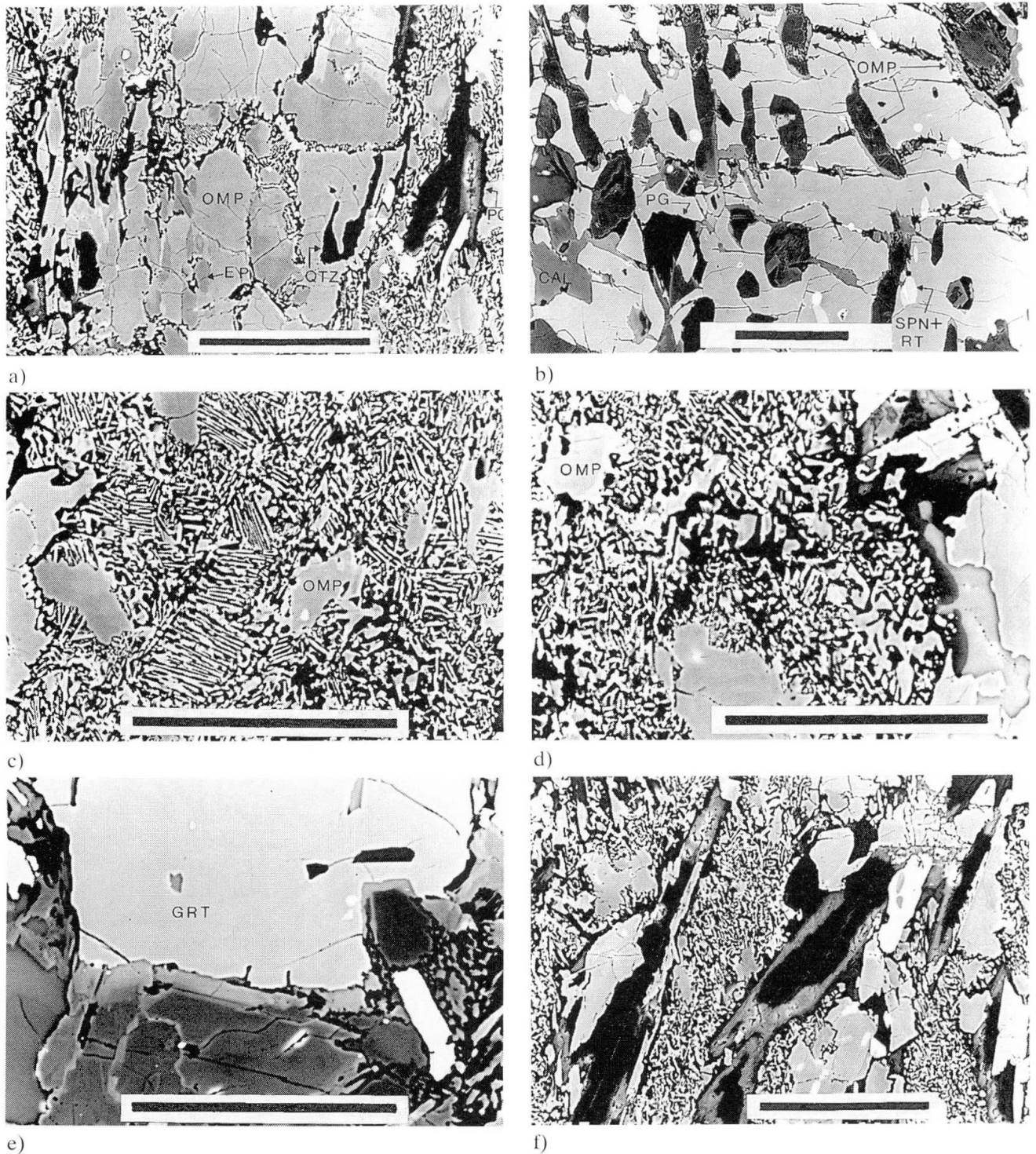


Fig. 2 Secondary electron images (WD = 39 mm, 20 kV, 20 nA) of relevant microtextures of Valosio eclogites. Bar is 100  $\mu\text{m}$ .

A) Foliated (vertical trend) eclogite showing omphacite (light grey), epidote (dark grey), quartz (black) and paragonite (black, right side). Omphacite is partially replaced by symplectite.

B) Garnet (light grey) displaying multiphase inclusion trails connected by veins. Omphacite is rimmed by pargasite; calcite, paragonite, aggregates of rutile and sphene are also present.

C) Diopside-plagioclase symplectite (Symp 1) with relics of omphacite.

D) Hornblende-plagioclase symplectite (Symp 2); relics of omphacite and Symp 1 are in the upper left corner.

E) Hornblende (dark grey) with a thin rim of pargasite amphibole (grey) developed after garnet (light grey).

F) Paragonite flakes (dark) rimmed by epidote (light grey) in a symplectite matrix.

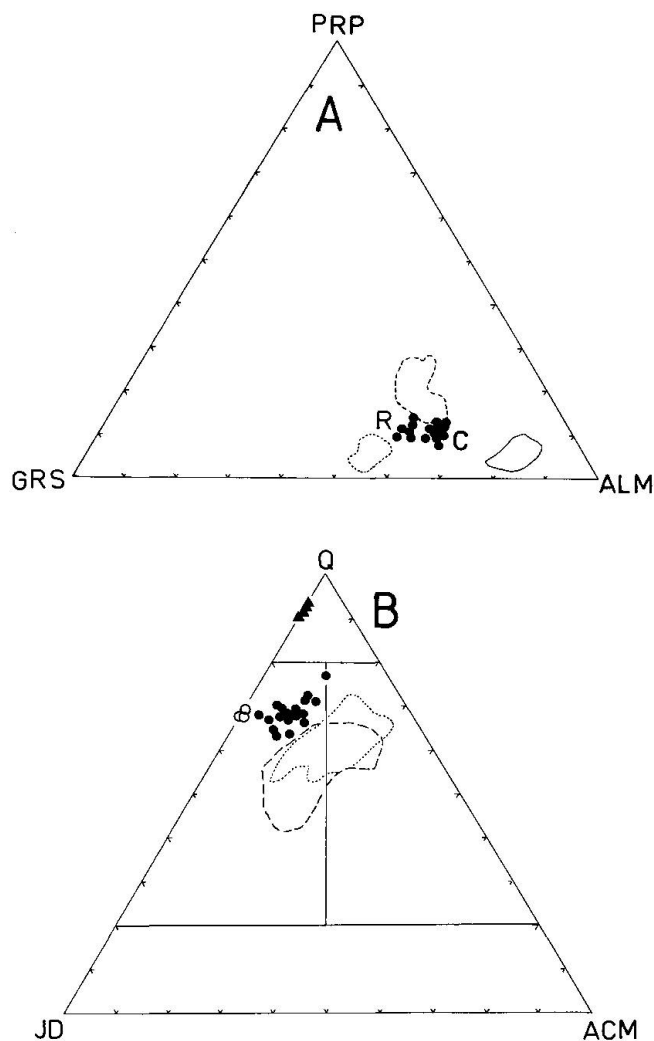


Fig. 3 A) Garnet composition of Valosio eclogites (C = core, R = rim). Dashed, solid and dotted enclosures represent the compositional fields for garnets from BCB (MESSIGA et al., 1992), eclogitic and retrograde garnets from Voltri massif eclogites (MESSIGA and SCAMBELLURI, 1991), respectively.

B) Clinopyroxene compositions of Valosio eclogites: full dots = omphacite porphyroclasts; open dots = porphyroclasts rims towards quartz; full triangles = clinopyroxene from Symp 1. Enclosures represent omphacite compositions from Voltri massif eclogites (MESSIGA and SCAMBELLURI, 1991); dashed enclosure = coronites, dotted enclosure = tectonites.

vein network connecting the larger part of the solid multiphase inclusions.

### Mineral chemistry

Mineral analyses were produced using a JEOL JXA-840A electron probe microanalyzer at "Centro Grandi Strumenti" (University of Pavia). WDS and EDS spectrometers simultaneously col-

lect X-ray intensities; operating conditions were: - accelerating voltage = 20 kV; - sample current = 20 nA; - detection limit = 0.01 wt%. Minerals were used as standards. Representative electron microprobe analyses (EMPA) are reported in table 1.  $\text{Fe}^{3+}$  contents for garnet were calculated assuming 8 cations and 12 oxygens in the formula unit.  $\text{Fe}^{3+}$  contents in clinopyroxenes and amphiboles were estimated by the method of LINDSLEY (1983), and of LAIRD and ALBEE (1981), respectively.

### Garnet

Garnet cores ( $\text{grt}_1$ ) are almandine-rich (56%–65%), with appreciable amounts of grossular (23%–35%). The pyrope content ranges from 6.6% to 9.2%, while spessartine is lower than 2.6% (Fig. 3A). The neoblastic rims of porphyroblasts ( $\text{grt}_2$ ) shows Ca-increase, balanced by a concomitant Fe-decrease (to extent of ca. 0.2 a.p.f.u.); Mn and Mg do not display significant variations.

### Clinopyroxene

Clinopyroxenes plot in the omphacite and in the QUAD fields (Fig. 3B), according to I.M.A. classification (MORIMOTO, 1988). Omphacite displays variable amounts in jadeite content (12%–33%), whereas the aegirine content is lower than 13%. In particular, the lowest aegirine contents were observed at the contact with quartz. Clinopyroxenes from Symp 1 are diopsides with ca. 10% of jadeite content.

### Amphibole

The classification scheme of LEAKE (1978) was adopted. The analysis of zoned amphiboles show two distinct compositional trends: i) a glaucophane-hornblende trend resulting from zoned grains retaining glaucophane relics; ii) a pargasite-hornblende trend characterizing the retrograde coronas around garnets (Figs 4 A, B, C, D). Amphiboles developed as thin rims around the solid inclusions and in veins cutting garnet porphyroblasts belong to the latter trend. Furthermore, actinolite rims hornblende porphyroblasts.

The glaucophane composition is defined by a JD ( $\text{NaAlCa}_1\text{Mg}_{-1}$ ) substitution higher than 1.4, with an upper limit of 1.8; the ED ( $\text{NaAlSi}_{-1}$ ) substitution is absent and the  $\text{MgFe}_{-1}$  substitution is about 0.6.

The compositional gap between Na- and Na-Ca-amphiboles (UNGARETTI et al., 1983) is evident (Fig. 4A). In fact, the JD substitution in hornblendes is never higher than 0.7, whereas ED and TK ( $\text{Al}_2\text{Mg}_{-1}\text{Si}_{-1}$ ) substitutions respectively range from 0.2 to 0.5 and from 0.1 to 0.4. The  $\text{MgFe}_{-1}$

Tab. 1 Representative microprobe analyses of mineral phases from mafic rocks of the Valosio massif. Garnets: 21 = porphyroblast core; 28 = porphyroblast rim. Clinopyroxenes: 29 = omphacite porphyroblast core; 35 = omphacite porphyroblast rim; 64 = omphacite porphyroblast rim towards quartz; 147 = clinopyroxene in symplectite. Amphiboles: 13 = pargasite in garnet inclusions; 89 = pargasite rimming garnet; 116 = glaucophane porphyroblast; 5 = hornblende porphyroblast; 118 = hornblende rimming glaucophane; 151 = hornblende in symplectite; 7 = tremolite in symplectite. Plagioclases: 39 = veins in garnet; 149 = in symplectite with hornblende; 143 = in symplectite with tremolite; 11 = paragonite; 46, 84 = epidote. Hyphens represent values under the detection limit of the electron microprobe.

|                                | GARNETS |        | CLINOPYROXENES |        |       |        | AMPHIBOLES |       |       |       |
|--------------------------------|---------|--------|----------------|--------|-------|--------|------------|-------|-------|-------|
|                                | 21      | 28     | 29             | 35     | 64    | 147    | 13         | 89    | 116   | 5     |
| SiO <sub>2</sub>               | 37.83   | 38.25  | 53.85          | 55.93  | 56.24 | 54.33  | 42.27      | 35.18 | 57.10 | 49.74 |
| TiO <sub>2</sub>               | —       | 0.15   | —              | —      | —     | —      | 0.31       | 0.08  | —     | —     |
| Al <sub>2</sub> O <sub>3</sub> | 21.22   | 21.63  | 4.96           | 7.91   | 10.37 | 3.70   | 15.12      | 19.79 | 11.82 | 8.86  |
| Cr <sub>2</sub> O <sub>3</sub> | —       | 0.02   | —              | —      | —     | —      | 0.01       | 0.04  | —     | —     |
| FeO <sub>tot</sub>             | 29.42   | 25.81  | 10.89          | 8.71   | 5.74  | 8.42   | 20.05      | 25.85 | 10.09 | 12.14 |
| MnO                            | 1.03    | 0.53   | 0.15           | —      | —     | —      | 0.41       | 0.35  | —     | 0.18  |
| MgO                            | 1.77    | 2.07   | 9.05           | 7.76   | 7.18  | 12.63  | 7.32       | 2.08  | 11.05 | 14.88 |
| CaO                            | 9.22    | 11.66  | 16.58          | 14.14  | 13.75 | 19.97  | 8.64       | 11.19 | 1.37  | 9.69  |
| Na <sub>2</sub> O              | 0.11    | —      | 4.49           | 6.17   | 6.32  | 1.70   | 4.34       | 3.02  | 6.28  | 2.87  |
| K <sub>2</sub> O               | —       | —      | —              | —      | —     | —      | 0.14       | 0.12  | —     | 0.07  |
| Tot.                           | 100.49  | 100.12 | 99.97          | 100.62 | 99.60 | 100.75 | 98.61      | 97.70 | 97.71 | 98.43 |
| N. of Ox.                      | 12      | 12     | 6              | 6      | 6     | 6      | 23         | 23    | 23    | 23    |
| Si                             | 2.99    | 3.00   | 1.98           | 2.00   | 2.01  | 1.98   | 6.22       | 5.47  | 7.82  | 6.99  |
| Ti                             | —       | 0.01   | —              | —      | —     | —      | 0.03       | 0.01  | —     | 0.03  |
| Al                             | 1.98    | 2.00   | 0.25           | 0.33   | 0.44  | 0.16   | 2.62       | 3.63  | 1.91  | 1.59  |
| Cr                             | —       | —      | —              | —      | —     | —      | —          | 0.01  | —     | —     |
| Fe <sup>3+</sup>               | 0.02    | —      | 0.15           | 0.10   | —     | —      | 0.88       | 0.75  | 0.13  | 0.77  |
| Fe <sup>2+</sup>               | 1.92    | 1.70   | 0.19           | 0.17   | 0.17  | 0.26   | 1.58       | 2.61  | 1.03  | 0.59  |
| Mn                             | 0.07    | 0.04   | 0.01           | —      | —     | —      | 0.05       | 0.05  | —     | 0.01  |
| Mg                             | 0.21    | 0.24   | 0.49           | 0.42   | 0.38  | 0.69   | 1.61       | 0.48  | 2.26  | 3.02  |
| Ca                             | 0.78    | 0.98   | 0.65           | 0.54   | 0.53  | 0.78   | 1.36       | 1.86  | 0.20  | 1.37  |
| Na                             | 0.02    | —      | 0.32           | 0.43   | 0.44  | 0.12   | 1.24       | 0.91  | 1.67  | 0.84  |
| K                              | —       | —      | —              | —      | —     | —      | 0.03       | 0.24  | —     | 0.02  |
| Tot.                           | 7.99    | 7.98   | 4.04           | 3.99   | 3.98  | 3.99   | 15.62      | 16.00 | 15.02 | 15.23 |

|                                | AMPHIBOLES |       |       | PLAGIOCLASES |       |       | PARAGONITE | EPIDOTES |       |
|--------------------------------|------------|-------|-------|--------------|-------|-------|------------|----------|-------|
|                                | 118        | 151   | 7     | 39           | 149   | 143   | 11         | 46       | 84    |
| SiO <sub>2</sub>               | 48.53      | 53.23 | 55.98 | 46.09        | 66.22 | 68.55 | 47.77      | 38.94    | 38.69 |
| TiO <sub>2</sub>               | —          | 0.12  | —     | 0.01         | —     | —     | —          | —        | 0.01  |
| Al <sub>2</sub> O <sub>3</sub> | 7.92       | 4.72  | 1.51  | 34.60        | 17.37 | 19.09 | 40.36      | 32.80    | 27.93 |
| Cr <sub>2</sub> O <sub>3</sub> | 0.03       | —     | —     | —            | —     | —     | —          | —        | —     |
| FeO <sub>tot</sub>             | 11.88      | 11.61 | 9.47  | 0.04         | 0.75  | 0.30  | 0.44       | 2.09     | 9.32  |
| MnO                            | 0.16       | 0.11  | —     | —            | 0.07  | —     | —          | —        | 0.11  |
| MgO                            | 16.05      | 16.09 | 18.59 | 0.09         | 0.09  | 0.03  | 0.17       | 0.03     | —     |
| CaO                            | 11.11      | 11.16 | 11.97 | 17.45        | 5.12  | 0.42  | 0.25       | 24.91    | 23.61 |
| Na <sub>2</sub> O              | 2.42       | 1.42  | 0.66  | 1.43         | 9.60  | 11.52 | 7.92       | —        | —     |
| K <sub>2</sub> O               | —          | —     | —     | 0.06         | —     | —     | 0.24       | —        | —     |
| Tot.                           | 98.10      | 98.46 | 98.18 | 99.77        | 99.22 | 99.91 | 97.15      | 98.77    | 99.76 |
| N. of Ox.                      | 23         | 23    | 23    | 8            | 8     | 8     | 11         | 12.5     | 12.5  |
| Si                             | 6.87       | 7.47  | 7.81  | 2.12         | 2.96  | 3.00  | 2.99       | 2.96     | 3.04  |
| Ti                             | —          | 0.01  | —     | —            | —     | —     | —          | —        | 0.01  |
| Al                             | 1.3        | 0.78  | 0.25  | 1.88         | 0.92  | 0.99  | 2.98       | 2.94     | 2.53  |
| Cr                             | —          | —     | —     | —            | —     | —     | —          | —        | —     |
| Fe <sup>3+</sup>               | 0.91       | 0.52  | 0.31  | —            | 0.03  | 0.01  | —          | 0.13     | 0.61  |
| Fe <sup>2+</sup>               | 0.49       | 0.84  | 0.80  | —            | —     | —     | 0.02       | —        | —     |
| Mn                             | 0.02       | 0.01  | —     | —            | —     | —     | —          | —        | 0.01  |
| Mg                             | 3.39       | 3.36  | 3.87  | 0.01         | 0.01  | —     | 0.02       | —        | —     |
| Ca                             | 1.68       | 1.68  | 1.79  | 0.86         | 0.25  | 0.02  | 0.02       | 2.03     | 1.99  |
| Na                             | 0.66       | 0.39  | 0.18  | 0.13         | 0.83  | 0.98  | 0.96       | —        | 0.01  |
| K                              | —          | —     | —     | —            | —     | —     | 0.02       | —        | —     |
| Tot.                           | 15.34      | 15.06 | 15.01 | 5.00         | 5.00  | 5.00  | 7.01       | 8.06     | 8.22  |

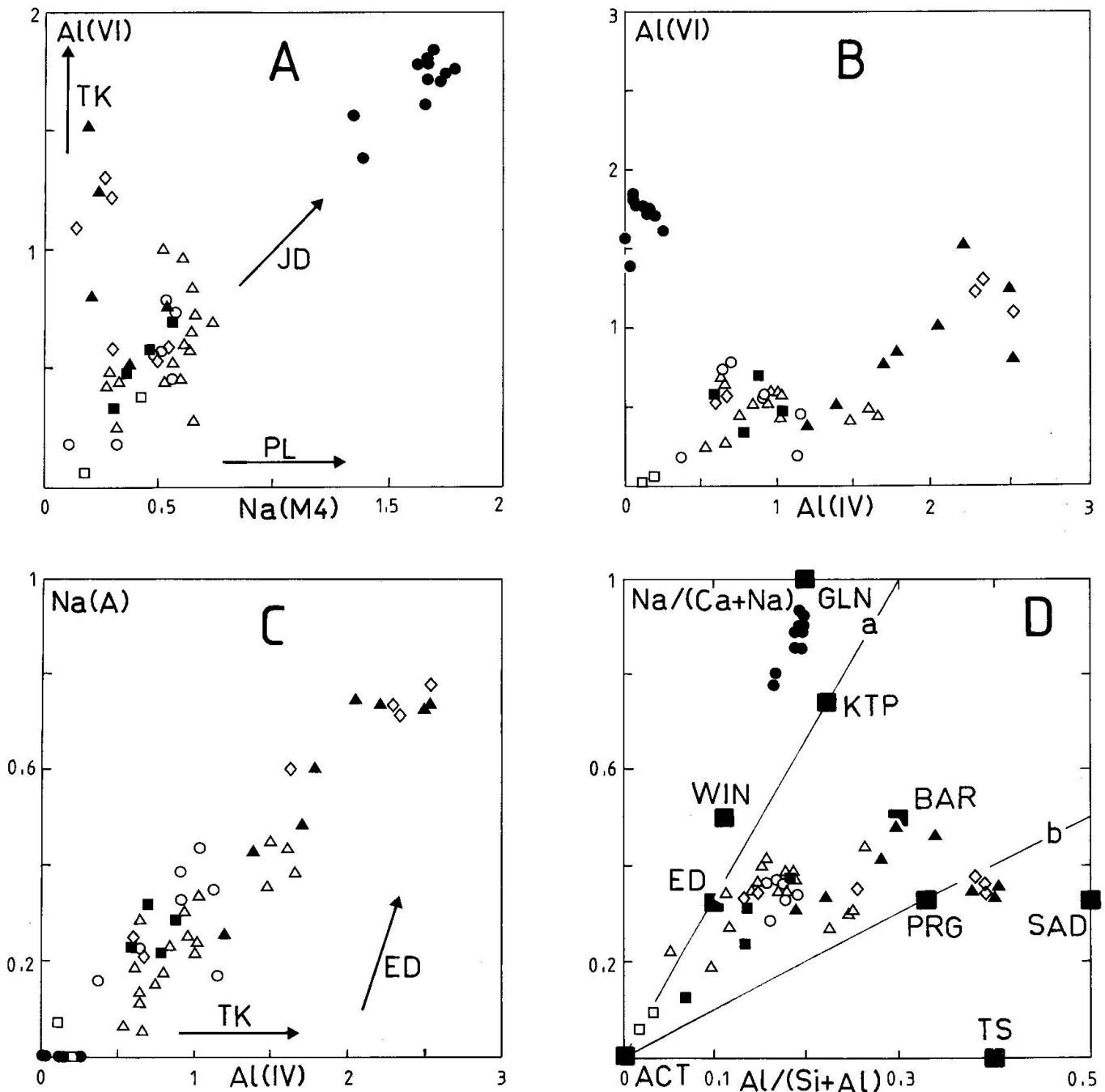


Fig. 4 Composition of amphiboles. Full circles = glaucophane porphyroblasts; open circles = hornblende rimming glaucophane; full squares = hornblende from Symp 2; open squares = tremolite from Symp 3; open triangles = hornblende porphyroblasts; full triangles = pargasite included in garnet; open diamonds = pargasite rimming garnet: A) plot of the Na(M4) vs the octahedral aluminium content (in a.p.f.u.), B) plot of tetrahedral vs octahedral aluminium content, C) plot of the tetrahedral aluminium content vs the sum of cations present in the A site. D) Variation in Na/Ca+Na with Al/Si+Al content. Lines (a) and (b) represent the trends for high pressure and medium pressure amphiboles, respectively (LAIRD and ALBEE, 1981).

substitution is in the 0.7–0.9 range. Indeed, according to the amphibole nomenclature (LEAKE, 1978), these amphiboles are termed actinolitic hornblendes, to hornblendes, to tschermakitic hornblendes, with increasing Al<sup>IV</sup>.

Blue-green amphibole in coronas after garnet are characterized by very high Al<sup>IV</sup> and Al<sup>VI</sup> (Fig. 4B) contents. The amphiboles closest to the garnet display elevated TK and ED substitutions (up to 1.5 and 0.8 respectively), and a very low JD



substitution (< 0.1). According to the classification of LEAKE (1978), these amphiboles are subsilicic pargasites to pargasites. A decrease of ED and TK (Fig. 4C) and a concomitant increase in JD substitution marks the transition to the outer part of the corona. Concerning the  $MgFe_{-1}$  substitution, it increases outwards from 0.2 to 0.6. The composition of the outermost coronitic amphiboles approaches that of hornblendes pertaining to the glaucophane-hornblende trend. Hornblende composition is also pointed out for the green amphibole porphyroblasts.

Hornblende generally characterize the amphiboles in the symplectites after omphacite and glaucophane, respectively. In terms of JD, TK and ED substitutions hornblendes from symplectites lie in the compositional field defined by the hornblendes in coronas and as porphyroblasts. In particular, the  $MgFe_{-1}$  substitution is rather high (ca. 0.8), similarly to hornblendes in the coronas around glaucophane.

Actinolitic amphiboles from symplectites after glaucophane displays very low value of JD, TK, and ED, but a high value for the  $MgFe_{-1}$  substitution (up to 0.9).

#### Plagioclase

The lowest An content (almost pure albite) is referred to the plagioclase-actinolite symplectites replacing glaucophane. Oligoclase ( $An_{20}$ ) is related to plagioclase in Symp 2 after omphacite. The lamellae width of Symp 1 prevent any correct microprobe analysis. Plagioclase occurring with pargasite in veins cutting garnet porphyroblasts displays the highest anorthite content ( $An_{54-87}$ ).

#### Paragonite

Paragonite composition does not show any compositional zoning and well approaches the stoichiometric formula. Based on 11 oxygens, the formula unit is characterized by very low values for  $Fe^{2+}$  (0.02–0.05 a.p.f.u.), Mg (< 0.05 a.p.f.u.), Ca (< 0.01 a.p.f.u.) and K (< 0.03 a.p.f.u.).

#### Epidote

The only major chemical variability appears to be in terms of  $Fe^{3+}/Al+Fe^{3+}$  ratio, gradually increasing from the core towards the rim of a single grain (from 0.03 to 0.2 a.p.f.u.).

### Metamorphic evolution

Because of the pervasive eclogitic deformation, the Valosio eclogites do not display any pre-eclogite relic. As a consequence, the protolith recognition and the reconstruction of the prograde

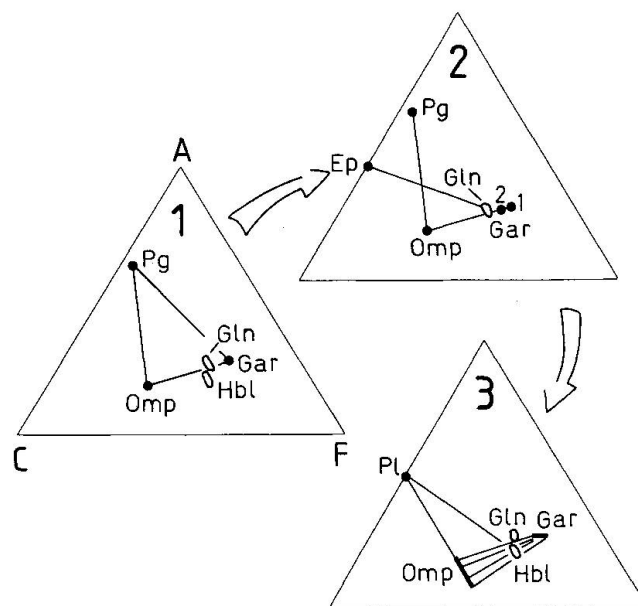
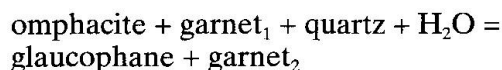


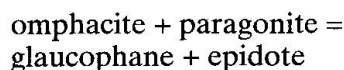
Fig. 5 Breakdown reactions controlling the transition from eclogite (1) to glaucophane (2) – and to hornblende (3) – bearing assemblages, using a NCMASH reference system and the ACF projection (THOMPSON, 1981). Due to its stability during the overall evolution (cf. Tab. 2), epidote is considered as an excess phase.

path cannot be ruled out. Moreover, the composition of eclogite minerals does not reflect a domain equilibrium recrystallization, but points out a wide chemical homogenization.

Table 2 reports the paragenetical sequence recognized on microtextural grounds. The omphacite + garnet ( $grt_1$ ) assemblage is firstly overgrown by a glaucophane + neoblastic garnet ( $grt_2$ ) assemblage; paragonite and rutile are overgrown by epidote and sphene, respectively. As a matter of fact, the glaucophane formation in these rocks is ruled by the breakdown of garnet-omphacite and omphacite-paragonite joins (Fig. 5). In the former case, the reaction:



explains the formation of Ca-enriched rims of neoblastic garnet (cf. GODARD et al., 1981). Similarly, the breakdown of omphacite-paragonite pairs due to the reaction:



accounts for the onset of glaucophane-bearing assemblages and testifies for the formation of the epidote rims around paragonite flakes. The Ca released during omphacite-garnet and/or omphacite-paragonite breakdown to glaucophane, is balanced either by neoblastic epidote, or by gros-

Tab. 2 Sequence of superposition of metamorphic assemblages in mafic rocks from Valosio massif.

| STAGES        | a     | b     |         | c       | d       |
|---------------|-------|-------|---------|---------|---------|
|               |       |       | (symp1) | (symp2) | (symp3) |
| garnet        | Grt 1 | Grt 2 |         |         |         |
| omphacite     |       |       |         |         |         |
| paragonite    |       |       |         |         |         |
| epidote       | Zo    |       |         |         |         |
| rutile        |       |       |         |         |         |
| glaucofane    |       |       |         |         |         |
| diopside      |       |       |         |         |         |
| sphene        |       |       |         |         |         |
| pargasite/Hbl |       |       |         |         |         |
| plagioclase   |       |       |         | Olig    | Ab      |
| actinolite    |       |       |         |         |         |

sular enrichment in garnet, or by sphene formation after rutile.

Some doubts could be expressed when trying to define the time relations between glaucophane and pargasite, as no overprinting microtextures have been observed. Since the rims of garnet porphyroblasts (grt<sub>2</sub>) are both grossular-enriched and partly overgrown by the pargasite coronas, glaucophane should predate pargasite. By contrast, the time relations between the glaucophane growth and the formation of diopside-plagioclase symplectites remain unclear. However, the formation of diopside-plagioclase symplectites after omphacite does not require the involvement of any other phase but omphacite (+qtz); this may testify that the pyroxene breakdown event occurs within the garnet stability field.

Metastable garnet-omphacite pairs may either give rise to amphibole coronas around garnet, or to the amphibole-plagioclase symplectites according to the following reactions:

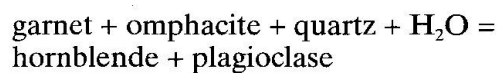
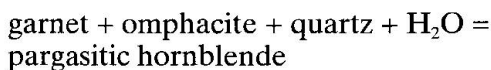


Figure 5 shows that plagioclase occurrence in these breakdown assemblages depends on the jadeite content of omphacite, as high jadeite contents would enhance a hornblende-plagioclase assemblage. The corona-forming reactions probably involve low jadeite pyroxenes, which determine the formation of a plagioclase-free amphibole assemblage.

The development of retrograde coronal amphibole is due to low-strain recrystallization driven by local fluid infiltration along grain boundaries. This mechanism determines a wide compositional scatter of amphibole which, in turn, is related to the composition of precursor eclogite minerals. As a consequence, the composition of amphiboles not only depends on pressure-temperature parameters, but also on their nucleation site. Figure 4D evidences a forked compositional trend of the Valosio retrograde amphiboles, with glaucophane and pargasite as end-member compositions and both trends converging towards

hornblende. Finally, actinolite matches the composition of later crystallized amphiboles.

The final decompressional stage is represented by the development of the actinolite-albite symplectites.

#### Thermobarometric estimates

Minimum pressure estimates of 1.2 GPa are inferred for the eclogite event, on the basis of the  $X_{Jd}$  (0.20–0.34) of omphacite coexisting with quartz (HOLLAND, 1983). An upper pressure limit of ca. 2.0 GPa is constrained by the stability of paragonite (HOLLAND, 1979). The ELLIS and GREEN (1979) calibration on the MgFe<sub>1</sub> exchange between garnet/omphacite pairs yields a temperature of  $530 \pm 50$  °C for the eclogite event (box a in Fig. 6A).

Pressure-temperature conditions pertaining to the decompressional stages have been evaluated on the basis of the different symplectite assemblages. According to the jadeite content in clinopyroxene (HOLLAND, 1983) a pressure estimate 0.9 GPa has been obtained for the diopside-plagioclase symplectite.

The thermobarometric estimates of the later decompressional stages are based on coexisting amphibole-plagioclase pairs. In the current literature, geothermobarometers based on amphibole-plagioclase assemblages (SPEAR, 1980; PLYUSININA, 1982; HAMMARSTROM and ZEN, 1986; BLUNDY and HOLLAND, 1990) are matter of a scientific debate (HAMMARSTROM and ZEN, 1992; RUTHERFORD and JOHNSON, 1992; POLI and SCHMIDT, 1992), mainly concerning the role played by the Al-involving substitutions (e.g. ED, PL, TK). Moreover, the difficulties in the partitioning of Al<sup>IV</sup> and Al<sup>VI</sup> from microprobe analyses may affect the reliability of amphibole-plagioclase thermobarometers.

We used the experimental calibration of PLYUSININA (1982) and obtained pressure-temperature values in agreement with microtextural observations and mineral assemblages. It is worth noting that this calibration uses Al<sub>tot</sub> contents of amphiboles and is therefore independent on the method of analysis recalculation. The hornblende-plagioclase symplectites yield temperatures of 530 °C and pressure of ca. 0.4 GPa, whereas actinolite-albite symplectites give temperature of 470 °C and minimum pressures of 0.2 GPa. Decrease of pressure conditions agrees with the lower jadeite substitution (BROWN, 1977; UNGARETTI et al., 1983) from hornblende to actinolite.

Such evaluations allow us to outline the adiabatic decompressional path of figure 6A. The box (b) represent the following stages: glaucophane growth, formation of diopside-plagioclase sym-

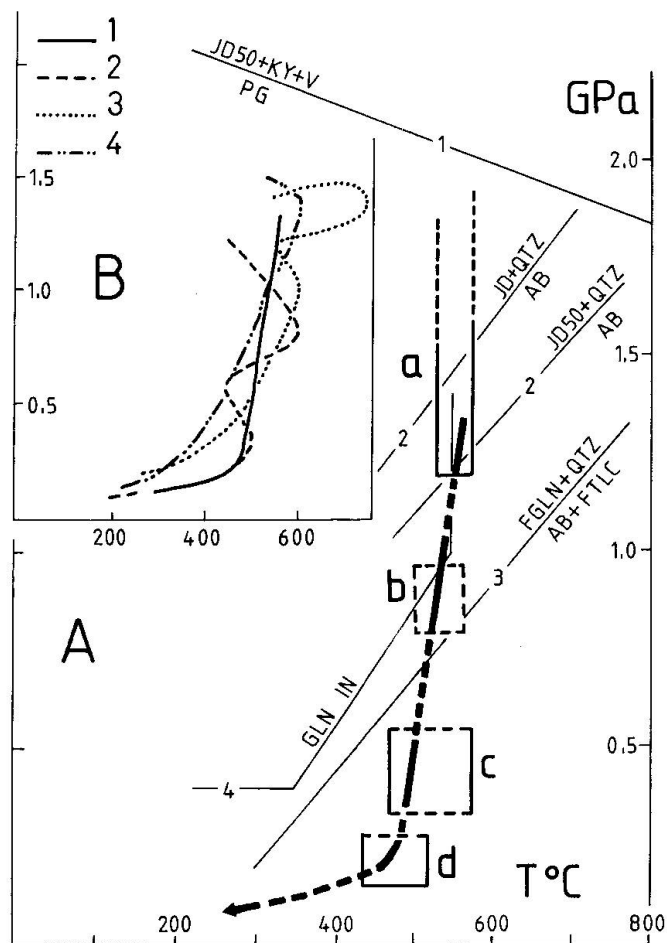


Fig. 6 A) Evolutionary P-T path of Valosio eclogites; boxes are referred to: eclogitic climax conditions (a); Symp 1, glaucophane, garnet veining (b); Symp 2 (c); Symp 3 (d). Curves labelled by numbers are referred to: 1) HOLLAND (1979); 2) HOLLAND (1983); MESSIGA and SCAMBELLURI (1991); 4) MARESCH (1977). B) General view on the P-T paths of the eclogitic terranes from Liguria (1 = Valosio; 2 = Voltri; 3 = Savona) and Dora Maira (4 = "cold" eclogitic unit).

plectites (Symp 1), and garnet veining. Boxes (c) and (d) represent the hornblende-plagioclase symplectites (Symp 2) and the growth of the actinolite-albite symplectite (Symp 3), respectively.

The Valosio eclogites experienced a superposition of decompressional stages, each marked by the onset of a given metamorphic reaction whose progress was fastly inhibited. The development of retrograde symplectites moreover suggests that reaction rates were slower than the rate at which P-T conditions were changing, i.e. the rate of uplift. This inference is supported by the high temperatures attained in the low pressure part of the P-T path.

### Discussion and conclusions

#### Comparison with other Ligurian eclogites

The comparison of evolutionary histories of rocks with similar bulk compositions (i.e. mafic eclogites) represents a key to correlate the eclogite-facies assemblages and the tectonometamorphic processes which occurred in different sectors of the Ligurian Alps (Valosio, Voltri and Savona massifs).

The high pressure stage within the Voltri and Valosio eclogites develops at comparable temperature conditions (ca. 500 °C; cf. MESSIGA et al., 1983; MESSIGA and SCAMBELLURI, 1991) and generates garnets with low pyrope content. On the other hand, the eclogite climax in the Variscan eclogites of the Savona crystalline occurs at much higher temperature conditions (ca. 620 °C; MESSIGA et al., 1992) producing garnet with higher contents of pyrope end member (MESSIGA et al., 1992).

The compositional evolution of amphiboles reveals a forked trend (Figs 7 A, B), which is a common feature to the three eclogite-facies terranes. In particular, the Voltri and Valosio eclogites record a similar amphibole evolution, the only significant difference being related to lower Na(M4) contents in the Valosio amphiboles (Fig. 7B). On the other hand, the Savona Variscan eclogites are characterized by: – a narrower compositional scatter of amphiboles; – the absence of glaucophane, i.e. the Na(M4) contents never exceed 0.6 a.p.f.u. In both Variscan and Alpine eclogites, the amphiboles replacing garnet display very high  $Al_{tot}$  contents matching subsilicic paragasite composition (MESSIGA et al., 1992). Secondary electron images combined with electron microprobe investigations suggest that the occurrence of such an amphibole-type can be due to disequilibrium recrystallizations driven by low diffusion rates (MESSIGA et al., in prep.).

The sequence of metamorphic assemblages and thermobarometric estimates thus suggests that the Valosio eclogites are related to the Alpine tectono-metamorphic event. The Valosio massif would represent the southernmost fragment of the Penninic Basement of the Western Alps. The inferred P-T path for the Valosio eclogites, however, is somewhat different from that reconstructed for the Voltri eclogites (Fig. 6B). The decompressional evolution of the Valosio eclogites point out an adiabatic path, as supported by thermobarometry and widespread development of symplectitic assemblages.

In the P-T path of the Voltri eclogites (MESSIGA and SCAMBELLURI, 1991), the pressure peak does not match the thermal climax, and the maxi-

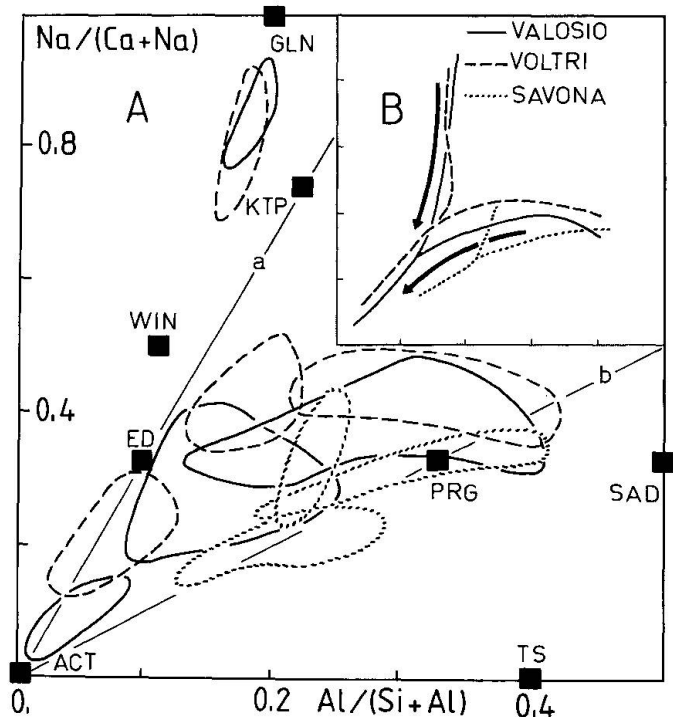


Fig. 7 A) Compositional fields for amphiboles from the different Ligurian eclogites. B) The forked trend is indicated by heavy arrows and represent a common feature.

imum temperature conditions are achieved during an early stage of the uplift. Subsequent temperature decrease is suggested by the appearance of glaucophane. The successive uplift to shallower levels is again accompanied by a temperature increase. Recently, SCAMBELLURI (1992) has substantiated by fluid inclusion microthermometry that the greenschist facies event occurs at high temperatures (500 °C) and relatively shallow depth (0.3 GPa). The complexity of the path drawn for the Voltri eclogites could be explained considering the thermal control exerted by tectonics during chronologically distinct thrusting events (MESSIGA and SCAMBELLURI, 1991).

The comparison between Variscan and Alpine metamorphic paths (Fig. 6B) highlights the higher temperatures attained during the Variscan orogenesis. Higher geothermal gradients during the Variscan exhumation have determined the absence of glaucophane and have enhanced a more pervasive chemical homogenization thus resulting in a narrow scatter of amphibole composition. On the contrary, the cooler Alpine exhumation has occurred through metastable equilibrations resulting in wider compositional changes of amphibole and in the diffuse presence of disequilibrium microtextures.

*Final remarks*

The Valosio eclogites can be considered as low temperature eclogites, according to the classification proposed by CARSWELL (1990). Their metamorphic evolution suggests fast changes in intensive variables due to high uplift rates. Fast exhumation would bring high temperature rocks at shallow levels, preventing their thermal equilibration at depth.

The Valosio eclogites display paragenetic and evolutionary similarities with the "cold" eclogite unit of the Dora Maira massif (cf. CHOPIN et al., 1991). The nearly adiabatic P-T path of the Valosio eclogites indicates fast uplift rates after the eclogite peak. The strong similarity between the low pressure parts of the evolutionary paths defined for the Voltri and Valosio massifs, implies that both units were probably juxtaposed only during the late decompressional stages, at less than 10 km depth. Before their junction, the units experienced different evolutions.

**Acknowledgements**

Thanks are due to an anonymous reviewer for constructive criticism. Microprobe facilities are supplied by the "Centro Grandi Strumenti, Università di Pavia". This work has been financially supported by Italian M.U.R.S.T.

**References**

- BELLINI, A. (1966): La geologia della zona di Monte Laione. *Atti Ist. Geol. Univ. Genova*, 4, 263–274.
- BLUNDY, J.D. and HOLLAND, T.B.J. (1992): Calcic amphibole equilibria and a new amphibole-plagioclase geothermometer. *Contrib. Mineral. Petrol.*, 104, 208–224.
- BROWN, E.H. (1977): The crossite content of Ca-amphiboles as a guide to pressure of metamorphism. *J. Petrology*, 18, 53–72.
- BRUNO, E. (1965): Ricerche petrografiche sugli scisti cristallini affioranti nella valle del Visone. *Atti Acad. Sc. Torino*, 99, 785–802.
- CABELLA, R., CORTESOGNO, L. and GAGGERO, L. (1991): Il basamento cristallino del Torrente Visone. *Rend. Soc. Geol. It.*, 14, 29–33.
- CARSWELL, D.A. (1990): Eclogites and eclogite facies: definition and classification. In: D.A. CARSWELL (ed.). *Eclogite facies rocks*. Blackie and Son Ltd. New York.
- CHIESA, S., CORTESOGNO, L., GALLI, M., MESSIGA, B., PASQUARÉ, G., PEDEMONTE, G.M., PICCARDO, G.B. and ROSSI, P.M. (1975): Assetto strutturale ed interpretazione geodinamica del Gruppo di Voltri. *Boll. Soc. Geol. It.*, 94, 555–581.
- CHOPIN, C., HENRY, C. and MICHARD, A. (1991): Geology and petrology of the coesite-bearing terrain, Dora Maira massif, Western Alps. *Eur. J. Mineral.*, 3, 263–291.
- CORTESOGNO, L. (1984): Metamorfismo e magmatismo prealpini nel basamento e nel tegumento delle Alpi liguri. *Mem. Soc. Geol. It.*, 28, 79–94.
- CORTESOGNO, L. and GAGGERO, L. (1988): Variazione composizionale degli anfiboli funzione dell'evoluzione pressione-temperatura in rocce mafiche del basamento Brianzese ligure. *Rend. Soc. Geol. It.*, 11, 183–188.
- DEL MORO, A., PARDINI, G., MESSIGA, B. and POGGIO, M. (1981): Dati petrologici e radiometrici preliminari sui Massicci Cristallini della Liguria Occidentale. *Rend. Soc. It. Mineral. Petrol.*, 38, 73–87.
- ELLIS, D.J. and GREEN, D.H. (1979): An experimental study on the effects of Ca upon garnet-clinopyroxene Fe-Mg exchange equilibria. *Contrib. Mineral. Petrol.*, 71, 13–22.
- ERNST, W.G. (1976): Mineral chemistry of eclogites and related mafic rocks from the Voltri Group, Italy. *Schweiz. Mineral. Petrogr. Mitt.*, 56, 293–343.
- FORCELLA, F., MOTTANA, A. and PASQUARÉ, G. (1973): Il massiccio cristallino interno di Valosio (Gruppo di Voltri, Provincia di Alessandria). *Mem. Soc. Geol. It.*, 12, 485–528.
- GODARD, G., KIENAST, J.R. and LASNIER, B. (1981): Retrogressive development of glaucophane in some eclogites from "Massif Armorican" (East of Nantes, France). *Contrib. Mineral. Petrol.*, 78, 126–135.
- HAMMARSTROM, J.M. and ZEN, E-an (1986): Aluminium in hornblende: an empirical igneous geobarometer. *Am. Min.*, 71, 1297–1313.
- HAMMARSTROM, J.M. and ZEN, E-an (1992): Discussion of Blundy and Holland's (1990) "Calcic amphibole equilibria and a new amphibole-plagioclase geothermometer". *Contrib. Mineral. Petrol.*, 111, 264–266.
- HOLLAND, T.J.B. (1979): Experimental determination of the reaction paragonite = jadeite + kyanite + water, and internally consistent thermodynamic data for part of the system Na<sub>2</sub>O-Al<sub>2</sub>O<sub>3</sub>-SiO<sub>2</sub>-H<sub>2</sub>O, with application to eclogites and blueschists. *Contrib. Mineral. Petrol.*, 68, 293–301.
- HOLLAND, T.B.J. (1983): The experimental determination of activities in disordered and short-range ordered jadeitic pyroxenes. *Contrib. Mineral. Petrol.*, 82, 214–220.
- KRETZ, R. (1983): Symbols for rock-forming minerals. *Am. Mineral.*, 68, 277–279.
- LAIRD, J. and ALBEE, A.L. (1981): Pressure, temperature and time indicators in mafic schistes: their application in reconstructing the polymetamorphic history of Vermont. *Am. J. Sci.*, 281, 127–175.
- LEAKE, B.E. (1978): Nomenclature of amphiboles. *Canad. Mineral.*, 16, 501–520.
- LINDSLEY, D.H. (1983): Pyroxene thermometry. *Am. Mineral.*, 68, 477–493.
- MARESCH, W.V. (1977): Experimental studies on glaucophane: an analysis of the present knowledge. *Tectonoph.*, 43, 109–125.
- MESSIGA, B. (1981): Evidenze strutturali e paragenetiche dell'evoluzione polifasica pre-alpina del Massiccio Cristallino di Savona. *Rend. Soc. It. Mineral. Petrol.*, 37, 739–754.
- MESSIGA, B. (1987): Alpine metamorphic evolution of Ligurian Alps (North-West Italy): chemography and petrological constraints inferred from metamorphic climax assemblages. *Contrib. Mineral. Petrol.*, 95, 269–277.
- MESSIGA, B., CORTESOGNO, L. and PEDEMONTE, G.M. (1975): Caratteri del metamorfismo alpino su rocce

- del Cristallino Savonese sottostanti la Falda di Montenotte. *Boll. Soc. Geol. It.*, 94, 1659–1683.
- MESSIGA, B., OXILIA, M., PICCARDO, G.B. and VANOSSI, M. (1981): Fasi metamorfiche e deformazioni alpine nel Brianzonese e nel pre-Piemontese-Piemontese esterno delle Alpi Liguri: un possibile modello evolutivo. *Rend. Soc. It. Mineral. Petrol.*, 38, 261–280.
- MESSIGA, B., PICCARDO, G.B. and ERNST, W.G. (1983): High pressure eo-alpine parageneses developed in Mg-metagabbros, Gruppo di Voltri, Western Liguria, Italy. *Contrib. Mineral. Petrol.*, 83, 1–15.
- MESSIGA, B. and SCAMBELLURI, M. (1991): Retrograde P-T-t path for the Voltri Massif eclogites (Ligurian Alps, Italy): some tectonic implications. *J. Metam. Geol.*, 9, 93–109.
- MESSIGA, B., TRIBUZIO, R. and CAUCIA, F. (1992): Amphibole evolution in variscan eclogite-amphibolites from the Savona crystalline massif (Western Ligurian Alps, Italy): controls on the decompressional P-T-t path. *Lithos*, 27, 215–230.
- MORIMOTO, N. (1988): Nomenclature of pyroxenes. *Mineral. Mag.*, 52, 535–550. *Schweiz. Mineral. Petrogr. Mitt.* 68, 95–111.
- PLYUSNINA, L.P. (1982): Geothermometry and geobarometry of plagioclase-hornblende-bearing amphibolites. *Contrib. Mineral. Petrol.*, 80, 140–146.
- POLI, S. and SCHMIDT, M.W. (1992): A comment on "Calcic amphibole equilibria and a new amphibole-plagioclase geothermometer" by J.D. BLUNDY and T.J.B. HOLLAND (*Contrib. Mineral. Petrol.* [1990] 104, 208–224). *Contrib. Mineral. Petrol.*, 111, 273–282.
- RUBIE, D.C. (1990): Role of kinetics in the formation and preservation of eclogites. In: D.A. CARSWELL (ed.). *Eclogite facies rocks*. Blackie and Son Ltd. New York.
- RUTHERFORD, M.J. and JOHNSON, M.C. (1992): Comment on Blundy and Holland's (1990) "Calcic amphibole equilibria and a new amphibole-plagioclase geothermometer". *Contrib. Mineral. Petrol.*, 111, 266–268.
- SCAMBELLURI, M. (1992): Retrograde fluid inclusions in eclogitic metagabbros from the Ligurian Western Alps. *Eur. J. Mineral.*, 4, 1097–1112.
- SPEAR, F.S. (1980): NaSi-CaAl exchange equilibrium between plagioclase and amphibole. *Contrib. Mineral. Petrol.*, 72, 33–41.
- THOMPSON, J.B. (1981): An introduction to the mineralogy and petrology of the biopyroxenes. In: "Amphiboles and other hydrous pyroxenes", VEBLEN, D. ed., *Reviews in Mineralogy*, Mineral. Soc. of America, 9A, 141–186.
- UNGARETTI, L., LOMBARDO, B., DOMENEGHETTI, C. and ROSSI, G. (1983): Crystal-chemical evolution of amphiboles from eclogitised rocks of the Sesia-Lanzo Zone, Italian Western Alps. *Bull. Mineral.*, 106, 645–672.
- VANOSSI, M. (1980): Les unités géologiques des Alpes Maritimes entre l'Ellero et la Mer ligure: un aperçu magmatique. *Mem. Soc. Geol. Padova*, 34, 101–142.
- VANOSSI, M., MESSIGA, B. and PICCARDO, G.B. (1980): Hypothèses sur l'évolution tectogénétique des Alpes ligures. *Rev. Geol. Dyn. et Geogr. phys.* 22, 3–13.
- VANOSSI, M., CORTESOGNO, L., GALBIATI, B., MESSIGA, B., PICCARDO, G.B. and VANNUCCI, R. (1984): Geologia della Alpi Liguri: dati, problemi, ipotesi. *Mem. Soc. Geol. It.*, 28, 5–75.

Manuscript received June 22, 1992; revised manuscript accepted September 19, 1992.